Dielectric and Morphological Studies on Polyester/Nanosilica Fume Composites

S. L. Abd-El Messieh,[1] Nehad N. Rozik[2]

[1]*Microwave Physics and Dielectrics Department, National Research Centre, Dokki, Cairo, Egypt*
[2]*Polymers and Pigments Department, National Research Centre, Dokki, Cairo, Egypt*

ABSTRACT: Styrenated polyester nanocomposites are a class of polymers reinforced with low quantities of well-dispersed nanoparticles with the aim of offering advantages over conventional composites. Nanosilica fumes with different particle sizes were used as a filler to form polyester nanocomposites. The average particle size was detected with transmission electron microscopy. We used the electrical properties [permittivity (ε'), dielectric loss (ε''), and electrical conductivity (σ)] to investigate the variation of the properties of the polyester/nanosilica fume composites by varying the filler ratio and particle size as well. The ε', ε'', and σ values were found to increase with increasing filler content up to a certain concentration, at which aggregation began to form and after which stability in these properties was attained. The second relaxation time (τ_2) associated with the orientation of the aggregates caused by the movement of the main chain was found to be unchanged up to a certain concentration of filler, after which a pronouncing increase in τ_2 was noticed. This result found further justification through the scanning electron micrographs. In addition, the values of σ, which were of the order of 10^{-11} S/cm, make the materials highly recommended for use for insulation purposes. © 2011 Wiley Periodicals, Inc. J Appl Polym Sci 122: 714–721, 2011

Key words: dielectric properties; electron microscopy; nanoparticle; particle size distribution; polyesters

INTRODUCTION

Organic/inorganic composite materials have been extensively studied for a long time. When the inorganic phases in organic/inorganic composites become nanosized, they are called *nanocomposites*.[1]

Polymer nanocomposites are potentially important because of the fact that they offer a number of significant advantages over traditional polymer composites. Conventional composites usually require a high content of the filler phase to achieve the desired properties of the composite material. Nanocomposites can achieve the same properties with a much smaller amount of the filler, producing materials of lower density and higher processibility.[2–4]

During past decades, studies of polymer-based nanocomposites have extended the application of these materials to many new fields.[5] Recent progress, including in the electric,[6] optical,[7] magnetic,[8] and mechanical properties[9] of nanocomposites, has been widely reported in the literature.

Polyester nanocomposites[10] are a class of polymers reinforced with low quantities of well-dispersed nanoparticles that offer advantages over conventional composites. Research on polymeric nanocomposite dielectrics has been conducted for several years. It has been proven that when the sizes of nanofillers are very small (when at least one of their dimensions is under 100 nm), the interface regions are so large that they start to interact at very low levels of loadings. Nanoparticles have great effects on the properties and morphology of polymeric nanocomposites because of their large specific surface and high surface energy. The interactions between the polymer matrix and nanoparticles alter the polymer chemistry, that is, the chain mobility and degree of cure, and generate new trap centers in the composite, which brings about a significant change in the electrical properties.[10,11]

In general, nanoparticles can be introduced to the polymer matrix in two different ways. Nanoparticles with functional units can be linked to the polymer backbone by chemical reactions,[12,13] whereas the blending process is favorable for commercial reasons.[14–19]

Unsaturated polyesters are widely used in the composite industry.[20,21] They can provide excellent mechanical, electrical, and chemical properties and good chemical and weather resistance.[21]

Polymer matrix nanocomposites can be prepared by the dispersion of a small amount of nanometer-size filler within the host medium. Polymer matrix/ nanocomposites exhibit three different configurations:

TABLE I
Technical Analysis: Melting-Aided Roasted Filter Aid

	CY-10	CY-1000	CY-H900	EG
Color	Pink	White	Pink	White
Description	Calcined filter aid	Flux-calcined filter aid	Flux-calcined filter aid	—
Loss on ignition	$\leq$3%	$\leq$3%	$\leq$3%	—
Bulk density (g/cm^3)	0.40	0.47	0.48–0.52	0.15–0.25
SiO$_2$	$\geq$90%	$\geq$89.60%	$\geq$85%	92–95%
Al$_2$O$_3$	$\leq$4%	$\leq$4%	$\leq$4%	$\leq$1.0%
Fe$_2$O$_3$	$\leq$1.5%	$\leq$1.5%	$\leq$1.5%	0.5–2.0%
CaO	$\leq$0.6%	$\leq$0.6%	$\leq$0.6%	$\leq$0.5%
MgO	$\leq$0.5%	$\leq$0.5%	$\leq$0.5%	$\leq$1.0%
Others	$\leq$0.4%	$\leq$0.8%	$\leq$0.8%	1–2%
Pb (mg/kg)	$\leq$1	$\leq$1	$\leq$1	—
Arsenite (mg/kg)	$\leq$1	$\leq$1	$\leq$1	—
Heavy metal	<0.005%	<0.005%	—	—

(1) microphase-separated composites, where the polymer matrix and nanofiller remain immiscible; (2) intercalated structures, where the polymer molecules are inserted between the nanofiller particles; and (3) exfoliated structures, where individual particles are dispersed in the polymer matrix. Polymer matrix nanocomposites are expected to be useful in replacing conventional insulating materials, providing tailored performance, by simply controlling the type and the concentration of nanoinclusions.[22–25] *Nanodielectrics* is a rather new term associating dielectrics with nanotechnology.[22] Dielectric spectroscopy is a powerful tool for the investigation of molecular mobility, phase transitions, conductivity mechanisms, and interfacial effects in polymers and complex systems.[22]

The changes of the segmental motions of the nanocomposites can be analyzed by dielectric relaxation spectroscopy.[26,27] Furthermore, because the ionic conductivity and polarization effects caused by the (partial) blocking of mobile charge carriers in inhomogeneous materials strongly influence the dielectric spectra (Maxwell–Wagner–Sillars polarization), dielectric spectroscopy is suitable for investigating the micromorphology of the nanocomposites as well. On the other hand, gas transport measurements can be used to investigate the changes in the mobility and the packing structure of polymer chains because the diffusion coefficient of the gas molecules is related to the molecular mobility of the polymer materials.[28–31] In addition, the solubility and the concentration of the penetrates depends on the fraction of the free volume of the nanocomposites.

The aim of this study was to prepare polyester/silica fume nanocomposites with different particle sizes with the aim of investigating their morphological characteristics and dielectric properties. Also, the main task of our investigation was to increase the effective dielectric constant of the composite system without an unacceptably large increase in the dielectric loss (ε''). In addition, we aimed to employ the relaxation mechanisms that reflect the structure–properties relationships of the polyester-based nanocomposites to follow up the filler aggregation.

EXPERIMENTAL

Material

Unsaturated polyester resin, as a commercial clear polyester supplied by Eternal Chemical Co. (Kachsiung, Taiwan), was used as received. The supplied resin was dissolved in styrene monomer by weight (36–40%).

Fillers

The used fillers were obtained from Qingdao Chuanyi Diatomite Co., Ltd. (China; http://www.cn-diatomite.cn) in addition to the local one (EG), which was obtained from the Chemical Industry Co. Kema (Aswan, Egypt). This local filler is a byproduct from the reduction of high-purity quartz with coal in electric arc furnaces in the manufacture of ferrosilicon alloys and silicon metal, with the technical analysis listed in Table I.

Sample preparation

Polyester/silica fume nanocomposites with different particle sizes were prepared by the mixture of different ratios of each silica fume (0–25 wt %) with an unsaturated polyester/styrene mixture provided from Eternal Chemical Co. on a glass plate. Methyl ethyl ketone peroxide (1.5 wt %) was added as an initiator in all cases. Care was taken to control the uniform thickness of the film for all compositions. The film thickness ranged from 0.1 to 0.15 cm. The prepared composites were left at room temperature (25 ± 1°C) until curing occurred.
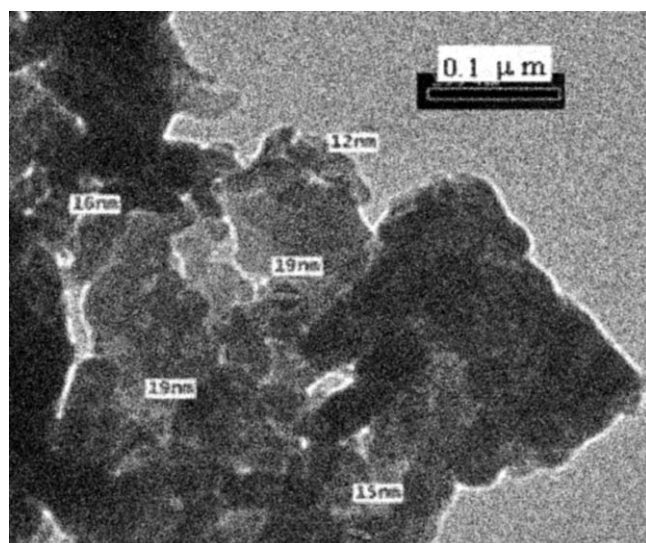
Figure 1 TEM micrograph for CY-H900.

Techniques

Dielectric measurements

Dielectric measurements were performed in the frequency range 100 Hz–100 kHz with an Inductance capacitance resistance meter LCR type AG-411 B (Ando Electric, Ltd., Tokyo, Japan). The capacitance, loss tangent, and resistance were obtained directly from the bridge from which the permittivity (ε'), ε'', and electrical conductivity (σ) were calculated.

A guard ring capacitor (type NFM/5T Wissenscaftlich Technische. Werkstatten GMBH, Weilheim, Germany) was used as a measuring cell. The cell was calibrated with standard materials,[32] and the experimental errors in ε' and ε'' were found to be ±3 and ±5%, respectively.

The temperature was controlled with an ultrathermostat. The experimental error in temperature control was ±0.1°C.

Scanning electron microscopy

The morphologies of the polyester composites with and without filler were examined with a scanning electron microscope (model JXA-840A, JEOL Technics, Tokyo, Japan). The magnification was 1000× for scanning electron observations with an applied voltage of 20 kV. The samples were coated with a thin layer of gold to ensure electron conductivity between the samples and the specimen stage.

Transmission electron microscopy (TEM)

Various fillers were examined with a JEOL JX 1230 technique with microanalyzer electron probe. This technique was used to determine the particle size of the investigated fillers.

RESULTS AND DISCUSSION

Particle size determination

TEM micrographs were used to determine the particle size of the fillers before impregnation in the polyester matrix. Figure 1 shows the TEM micrographs for CY-H900, from which the particle size was found to be in the range 12–19 nm, which indicated that the CY-H900 particles were in the nanoscale.

Figure 2 represents the TEM micrograph of the filler CY 1000, from which we observed that the particle size ranged from 26 to 40 nm, also in the nanoscale.

Figure 3 shows the TEM micrograph of the filler CY 10. Form this figure, we observed that the particle size of this filler ranged from 92 up to 114 nm, which was much larger than the previous two samples; that is, the size was on the border of nanoscale particles.

Figure 4 represents the TEM for the filler obtained from the chemical industry company Aswan Egypt. From this figure, it is clear that the particles were spherical in shape and the particle size was a combination of nanoscale and microscale, as it ranged from 38 to223 nm.

Dielectric measurements

ε' and ε'' were measured in the frequency range from 100 Hz up to 100 kHz and at 30°C for polyesters filled with CY-H900, CY1000, CY10, and the local one (EG), respectively, with different concentrations ranging from 0 to 20%. Two examples from the
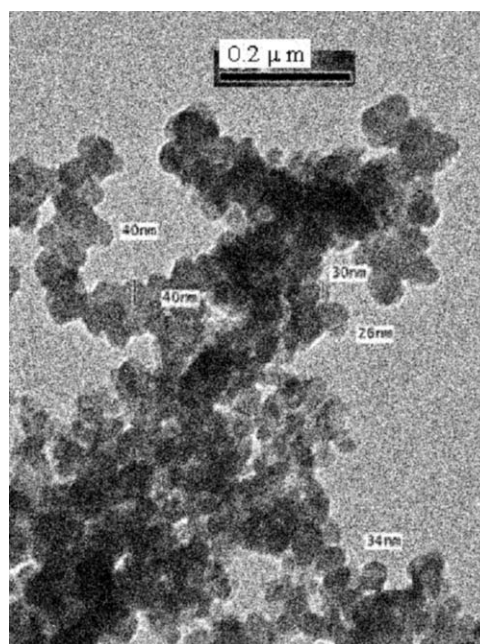

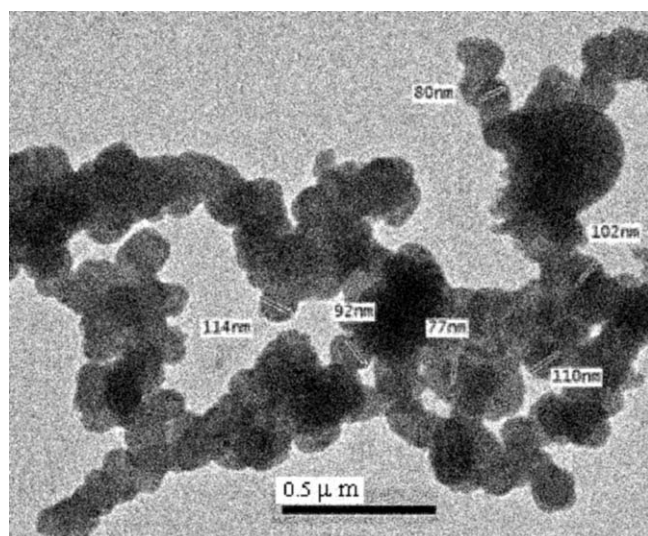**Figure 2** TEM micrograph for CY 1000.

Figure 3 TEM micrograph for CY 10.

measured data are given in Figure 5 for polyester filled with (a) EG and (b) CY-H900.

From this figure, it is clear that ε' increased with increasing percentage of filler, whereas it decreased with increasing applied frequency; this shows anomalous dispersion. On the other hand, a pronounced increase in ε' with increasing filler content was noticed. This increase seemed to be nonlinear and dependent on the filler particle size. To understand the dependence of ε' upon the filler content, Figure 6 depicts the variation of ε' versus filler content for the four types of fillers under investigation at a fixed frequency ($f = 100$ Hz).

From this figure, we observed that ε' increased dramatically with increasing filler content up to a certain concentration, after which this increase became very small. This increase was found to be on the order CY-H900 > CY100 > CY 10 > EG. This may have been due to the unhomogeneity of the filler distribution at higher loadings, which formed aggregation inside the polymeric matrix.[33] Also, it was seen that the dramatic increase in ε' began more quickly for the composites loaded with smaller size particles (4% for CY-H900 and CY100) compared with the bigger ones (6% for both CY 10 and EG). This was because as the particle size became small, the number of particles per unit volume increased, and consequently, an enhancement in the property was expected.[34]

As shown in Figure 5, the values of ε'' in the lower frequency were higher. These high values may have been a combination of direct-current (dc) conductivity resulting from the increase of ion mobility and the Maxwell–Wagner effect.[35] As the moving charge carriers were separated over a considerable distance, its contribution to the dielectric storage, by orders of magnitude, was larger than
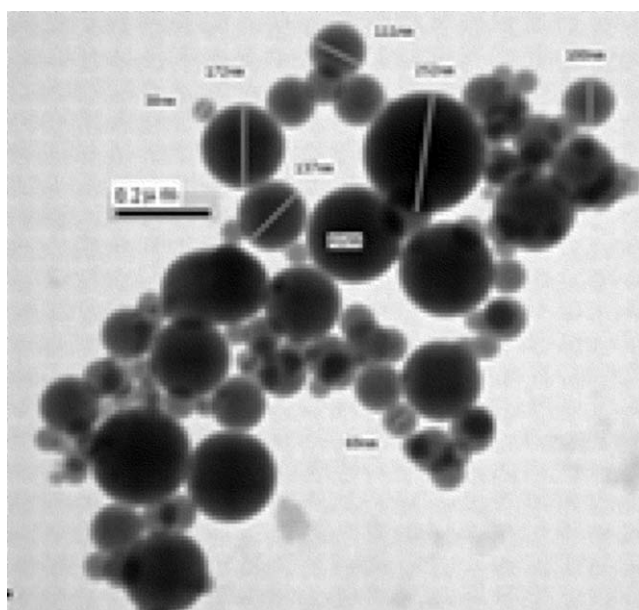

Figure 4 TEM micrograph for the local sample (EG).

that of the orientational polarization. This effect is generally accepted as a characteristic identifying Maxwell–Wagner polarization.[36]

Analysis of the absorption curves relating ε'' and the applied frequency after subtraction of the conductivity part was done in terms of two superimposed
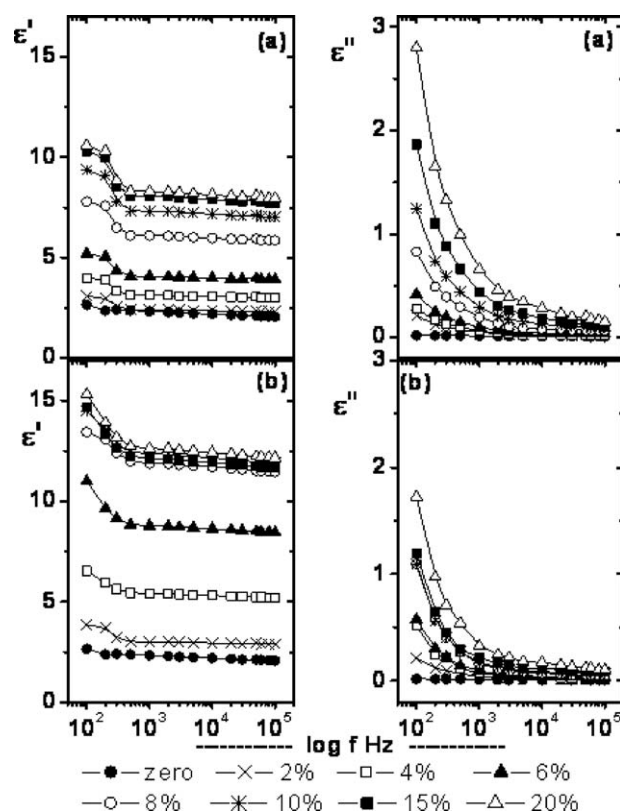

Figure 5 ε' and ε'' versus frequency for polyester filled with (a) EG and (b) CY-H900.
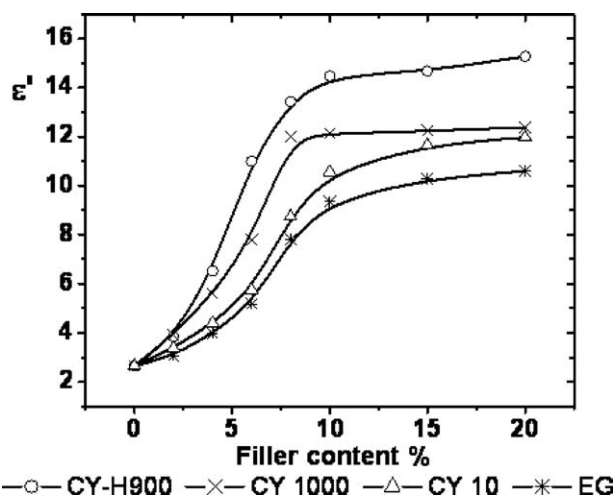
Figure 6 ε' at $f = 100$ Hz versus the filler content percentage.

processes based on Frohlich and Havriliak–Negami functions according to the equations given before.[32] After subtraction of the losses due to the dc conductivity, the first relaxation process, which was ascribed to the Maxwell–Wagner effect, was found to be on the order of 300 Hz and was unaffected by either filler loading or particle size. Its ε'' maximum frequency values were found to increase with increasing filler loading, as shown in Figure 7.

The second absorption region in the higher frequency range with the second relaxation time (τ_2) on the order of 10^{-5} could have been due to the orientation of the aggregates caused by the movement of the main chain. After a certain concentration of filler loading, depending on the particle size, the values of τ_2 were found to be shifted toward the lower frequency.

The increase in τ_2 reflected an increase in the rotating volume and, consequently, increases in the aggregation of filler particles. This aggregation lost the composite its profound impact as it negatively affected its dielectric properties. This finding is considered to be an explanation of the plateau noticed in the ε' values shown in Figure 6. So to get a composite characterized by its high performance insulating properties, the filler loading should not exceed 6% for both CYH900 and CY1000 and also should not exceed 8% for both CY10 and EG fillers.

Examples of the analyses for the polyester free from filler and that with 10% CY-H900 are illustrated graphically in Figure 8.

From this figure, it is clear that the second process was strongly affected by the filler loading and shifted toward lower frequency.

After subtraction of the losses due to both dc conductivity and the Maxwell–Wagner effect, the higher frequency region was clearly detected, as shown in Figure 9, for the polyesters loaded with CY-H900
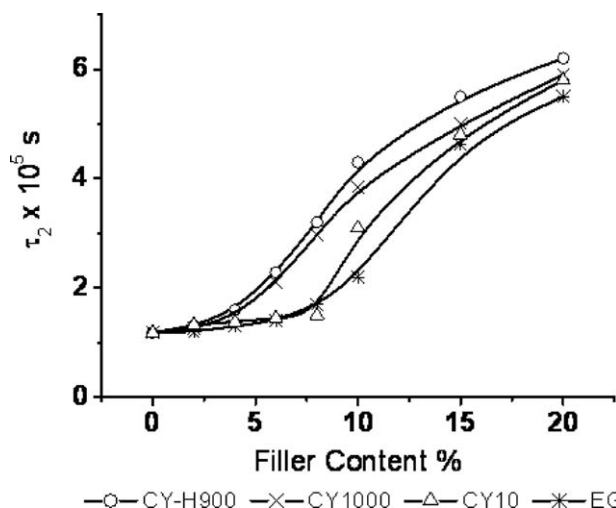
and CY10. In this figure, the shift in the maximum frequency (f_{m2}), and consequently, τ_2, is clear.

σ

σ calculated from the measured resistance is plotted graphically versus filler content in Figure 10. In this figure, it is interesting that σ for all of the composites was on the order of 10^{-11}, that is, in the range
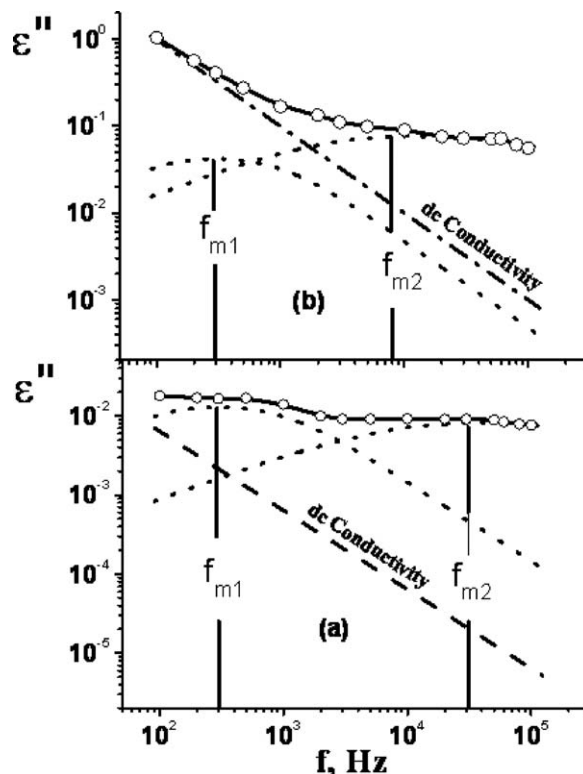

Figure 7 Relation between τ_2 and the filler content percentage.

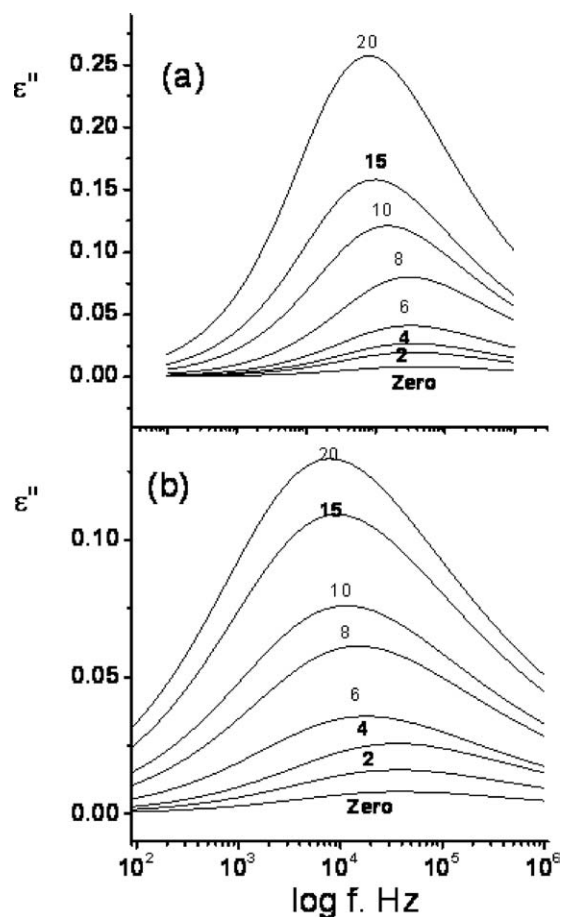**Figure 8** Example of the analyses for the polyesters (a) free from filler and (b) with 10% CY-H900.

Figure 9 Second relaxation process for the polyesters loaded with (a) CY 10 and (b) CY-H900.

suitable for insulation purposes.[37] Also, it is notable that σ increased with increasing filler content up to a certain concentration, at which aggregations began to be formed. After that, stability in σ was detected. This finding is considered to be further justification for those obtained for ε' and τ_2. Also, it is clear from the same figure that the values of σ were on the order of 10^{-11} S/cm, which is the range required for insulation purposes. This finding recommends these composites for use as insulation materials.

Scanning electron microscopy

Figure 11 represents the scanning electron micrograph of the composites containing 6 and 10% of each filler in addition to the polyester free from filler. From these micrographs, it is clear that excellent particle distribution of the filler was seen for composites containing 6%; this confirmed the performance of the insulation properties obtained before. It was also seen that the aggregation of filler particles was more detectable for composites containing 10% of the fillers; this is considered to be the main reason for the plateau noticed after such a concentration.
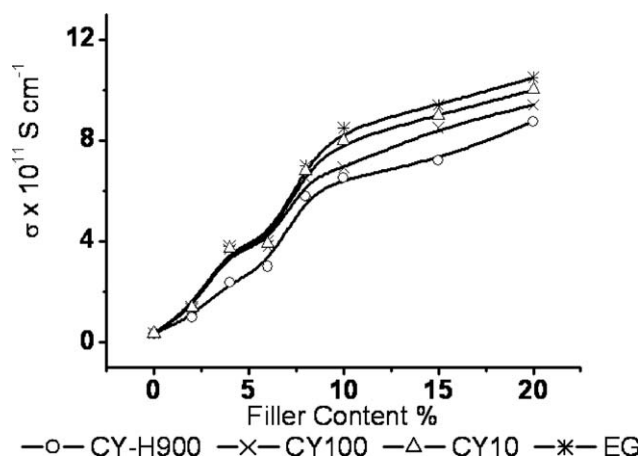

Figure 10 σ versus the filler content percentage.

CONCLUSIONS

From our investigation, we concluded that

The particle size of the four different types of silica fumes was determined with TEM. The results show that two of them were on the order of the nanoscale and one of them was at the border of nanoparticles, whereas the last one was a combination between the nano and macro ranges.

ε' and ε'' were measured at different frequencies for the composites of polyester with various contents of silica fumes, which acted as a filler. ε' was found to increase dramatically with increasing filler content until certain concentration, after which this increase became very small. On the other hand, ε' was found to increase with decreasing particle size of the filler.

ε'' increased with increasing filler content and decreased with applied frequency. This increase was promising only for composites containing less than 6% filler loading for both CY900 and CY1000 and 8% for both CY10 and EG as the ε'' values did not exceed 0.8; that is, insulating property performance was achieved.

The analyses of the curves relating ε'' to the applied frequency revealed two relaxation mechanisms. The first one, at the lower frequency range, which associated by the Maxwell–Wagner effect, was found to be unaffected either by the filler particle size or its content. The second relaxation mechanism (τ_2), associated with the orientation of the aggregates caused by the movement of the main chain, was found to be shifted toward the lower frequencies with increasing filler loading, depending on the particle size of the filler.

The values of σ were on the order of 10^{-11} S/cm, which is the range required for insulation purposes.

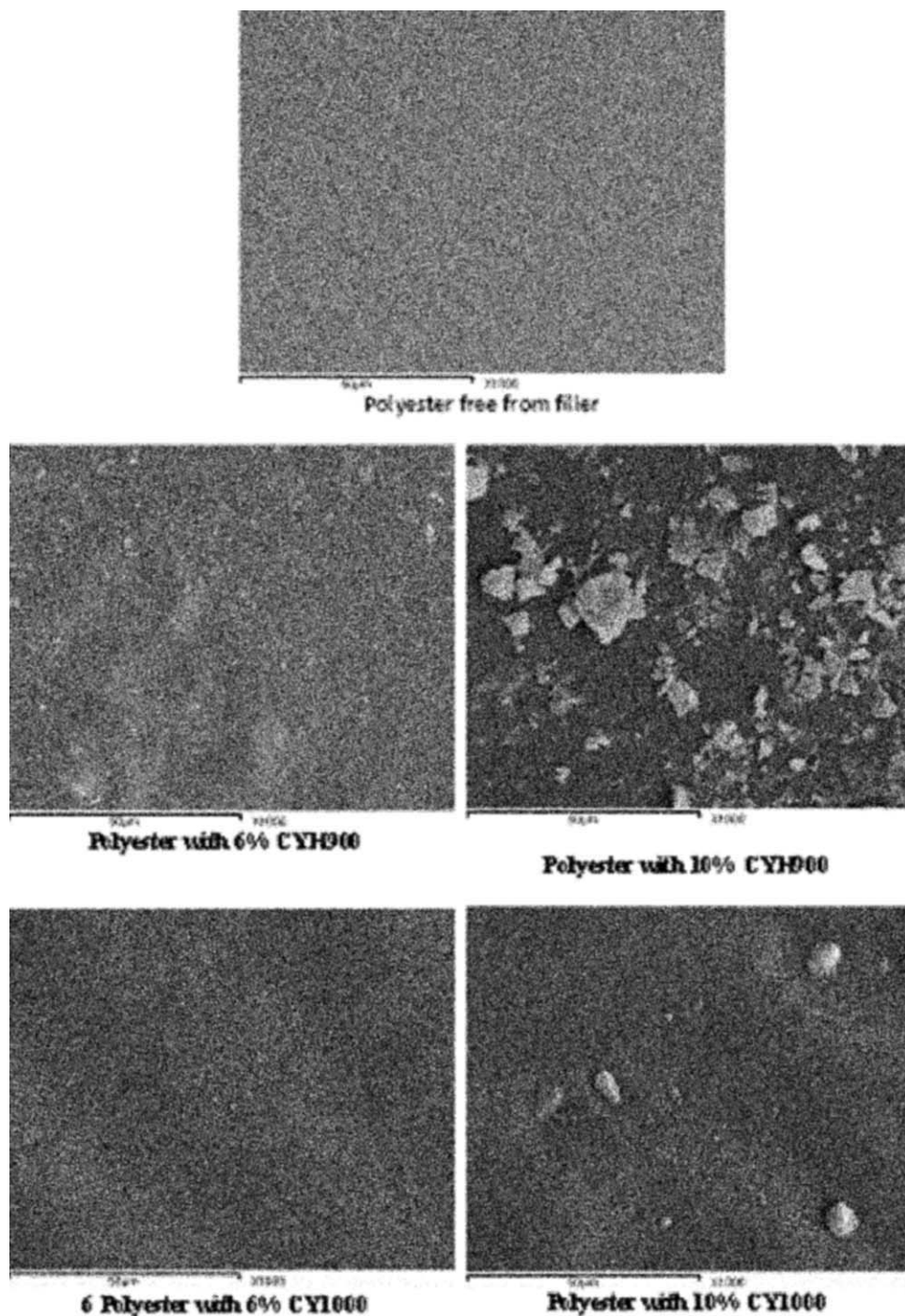The scanning electron micrographs indicated that fine distribution of filler was detected for the 6%

Figure 11 Scanning electron micrographs of the polyester composites with 6 and 10% of the fillers.

filler loading composites, whereas aggregate formation was clear for those containing 10% filler loading.

References

1. Zou, H.; Wu, S.; Shen, J. Chem Rev 2008, 108, 3893.
2. Chen, Y. C.; Wu, L. M. Prog Org Coat 2005, 54, 120.
3. Zhang, S. W.; Zhou, S. X.; Weng, Y. M.; Wu, L. M. Langmuir 2005, 21, 2124.
4. Edser, C. Plast Additives Compd 2002, 4, 30.
5. Ishida, H.; Campbell, S.; Blackwell, J. Chem Mater 2000, 12, 1260.
6. Chen, Q.; Zhao, L.; Li, C.; Shi, G. J Phys Chem C 2007, 111, 18392.
7. Guo, L.; Yang, S.; Yang, C. Chem Mater 2000, 12, 2268.
8. Tang, B. Z.; Geng, Y.; Lam, J. W. Y.; Li, B.; Jing, X.; Wang, X.; Wang, F.; Pakhomov, A. B.; Zhang, X. X. Chem Mater 1999, 11, 1581.
9. Burnside, S. D.; Giannelis, E. P. Chem Mater 1995, 7, 1597.
10. Gornicka, B.; Prociow, E. Acta Phys Pol A 2009, 115, 842.
11. Li, H.; Liu, G.; Liu, B.; C. Chen, S. Mater Lett 2007, 61, 1507.
12. Kawashima, D.; Aihara, T.; Kobayashi, Y.; Kyotani, T.; Tomita, A. Chem Mater 2000, 12, 3397.

13. Ono, Y.; Akiyama, M.; Suzuki, E. Chem Mater 1993, 5, 442.
14. Joshi, M.; Butola, B. S.; Simon, G.; Kukaleva, N. Macromolecules 2006, 39, 1839.
15. Kopesky, E. T.; McKinley, G. H.; Cohen, R. E. Polymer 2006, 47, 299.
16. Kopesky, E. T.; Haddad, T. S.; McKinley, G. H.; Cohen, R. E. Polymer 2005, 46, 4743.
17. Kopesky, E. T.; Haddad, T. S.; Cohen, R. E.; McKinley, G. H. Macromolecules 2004, 37, 8992.
18. Soong, S. Y.; Cohen, R. E.; Boyce, M. C.; Mulliken, A. D. Macromolecules 2006, 39, 2900.
19. Zhao, Y.; Schiraldi, D. A. Polymer 2005, 46, 11640.
20. Cao, X.; Lee, L. J. Polymer 2003, 44, 1893.
21. Peng, G. R.; Li, Q. S.; Yang, Y. L.; Wang, H. F.; Li, W. Polym Adv Technol 2008, 19, 1629.
22. Psarras, G. C.; Gatos, K. G.; Karahaliou, P. K.; Georga, S. N.; Krontiras, C. A.; Karger-Kocsis, J. Express Polym Lett 2007, 12, 837.
23. Tanaka, T.; Montari, G. C.; Mülhaupt, R. IEEE Trans Dielectr Electr Insulation 2004, 11, 763.
24. Montanari, G. C.; Fabiani, D.; Palmieri, F.; Kaempfer, D.; Thomann, R.; Mulhaupt, R. IEEE Trans Dielectr Electr Insulation 2004, 11, 754.
25. Pegoretti, A.; Dorigato, A.; Penati, A. Express Polym Lett 2007, 1, 123.
26. Kremer, F.; Schönhals, A. In Broadband Dielectric Relaxation Spectroscopy; Kremer, F., Schönhals, A., Eds.; Verlag: Berlin, 2002; Chapter 2, p 35.
27. Schönhals, A.; Kremer, F. In Broadband Dielectric Relaxation Spectroscopy; Kremer, F., Schönhals, A., Eds.; Springer: Berlin, 2002; Chapter 1, p 1.
28. Schönhals, A.; Kremer, F. In Broadband Dielectric Relaxation Spectroscopy; Kremer, F., Schönhals, A., Eds.; Springer: Berlin 2002; Chapter 3, p 59.
29. Lin, H.; Van Wagner, E.; Freeman, B. D.; Toy, L. G.; Gupta, R. P. Science 2006, 331, 639.
30. Merkel, T. C.; Freeman, B. D.; Spontak, R. J.; He, Z.; Pinnau, I.; Meakin, P.; Hill, A. J. Sorption Chem Mater 2003, 15, 109.
31. Yampolskii, Y. P.; Korikov, A. P.; Shantarovich, V. P.; Nagai, K.; Freeman, B. D.; Masuda, T.; Teraguchi, M.; Kwak, G. Macromolecules 2001, 34, 1788.
32. Abd-El-Messieh, S. L.; Abd-El-Nour, K. N. J Appl Polym Sci 2003, 88, 1613.
33. Dimitry, O. I. H.; Sayed, W. M.; Mazroua, A. M.; Saad, A. L. G. Polimery 2009, 54, 8.
34. Barber, P.; Balasubramanian, S.; Anguchamy, Y.; Gong, S.; Wibowo, A.; Gao, H.; Ploehn, H. J.; Zur Loye, H. C. Materials 2009, 2, 1697.
35. Rozik, N. N.; Abd-El Messieh, S. L.; Abd-El Nour, K. N. J Appl Polym Sci 2010, 115, 1732.
36. Steeman, P. A. M.; van Turnhout, J. In Broadband Dielectric Relaxation Spectroscopy; Kremer, F., Schönhals, A., Eds.; Springer: Berlin, 2002; Chapter 13, p 495.
37. Huang, J. C. Adv Polym Technol 2002, 21, 299.